

memorandum

date September 11, 2012 (Revised 1/4/13)

to Jim Johannessen (Coastal Geologic Services)

from Louis White, PE (CA)

subject Wave Climate, Sediment Transport, and Inlet Analysis for Swan Lake

1. Introduction

ESA PWA is assisting Coastal Geologic Services Inc. (CGS) to prepare an engineering feasibility assessment of restoring a tidal connection to Swan Lake as part of the Swan Lake Restoration Project for the Skagit Fisheries Enhancement Group (SFEG). This memorandum provides a summary of our work to describe the wave climate and sediment transport at the site, in addition to addressing inlet stability questions related to constructing a new tidal inlet connection to Swan Lake. The work described in this memorandum was completed by Louis White, To van Dang, Dane Behrens, and Doug George, with oversight by Bob Battalio, PE. Site measurements and other data, along with review and comments on this memo were provided by CGS.

1.1. Project Goals and Objectives

Recent efforts have been directed at identification of feasible restoration alternatives to improve estuarine and marine nearshore processes and fish passage into the site, including enhancing existing salt marsh vegetation and fish habitat for juvenile salmonids (CGS 2010). The goal of this study is to evaluate the feasibility of establishing a tidal connection by installing a culvert with self-regulating tide gates or by constructing a new open channel. This memorandum presents information pertinent to the wave climate, sediment transport, and the inlet analysis, which are intended to support continuing evaluation of the feasibility of restoring a tidal connection. The specific objectives of this memorandum are:

- To develop an understanding of the wave climate affecting the site, and to calculate the wave power exposure by wind waves and swell;
- To estimate the potential sediment transport rate driven by waves;
- To evaluate the stability and sustainability of a new tidal inlet at the north end of the site;
- To estimate the approximate equilibrium geometry of a new tidal inlet;
- To recommend a preliminary feasibility assessment of establishing a tidal connection to Swan Lake via a new open channel inlet or a culvert with self-regulating tide gates.

1.2. Background and Hydrologic Considerations

Swan Lake is a back-barrier, closed lagoonal marsh located on the western edge of Whidbey Island, Washington, on the Strait of Juan de Fuca (Figure 1). The site is exposed to locally generated wind waves and longer period swell from the Pacific Ocean that penetrates through the Strait of Juan de Fuca. The tide range at the site is approximately 7.5 feet between mean lower low water (MLLW) and mean higher high water (MHHW). Tidal datums at Swan Lake were estimated by CGS using the program VDatum (Table 1). The relationship between mean lower low water and NAVD was verified to within 0.5 ft using water level data collected on site. The elevations in this memorandum are presented in feet relative to MLLW.

Table 1. Tidal datums used for the Swan Lake wave and inlet analyses.

Tide	Elevation (ft MLLW)
Mean Higher High Water (MHHW)	7.5
Mean High Water (MHW)	6.8
Mean Tide Level (MTL)	4.6
Mean Sea Level (MSL)	4.6
Mean Low Water (MLW)	2.4
North American Vertical Datum of 1988 (NAVD)	0.3
Mean Lower Low Water (MLLW)	0.0

Source: CGS, data from VDatum

Swan Lake is currently connected to the Strait of Juan de Fuca by two culverts that drain the approximately 100 acre lake through flap gates. These culverts are located where the shoreline angle jogs from a bearing of approximately 15° to 45°, which is also a relatively short distance from the lake to deep water offshore (Figure 2). The culverts consist of two 30-inch inside diameter pipes, one of which was slip-lined with a 24-inch high density polyethylene (HDPE) inside, based on construction documents (Island County 2008) and discussions with Island County staff. The culverts run from the tide gate box on the seaward side of the road and out into the lower intertidal zone. The culverts run through an Island County easement, located between two residential properties. Local operators indicated that cobble sometimes deposits in the aluminum pipe, and sand often deposits in both pipes during the summer. Debris comprising small pieces of wood often clogs the flap gates which require approximately weekly maintenance.

Locations for the new culvert and new open channel inlet were selected to provide the best conditions for each alternative rather than at the same locations. The reasons are developed later in this memorandum, but are summarized here to describe the alternatives.

Culvert: The existing culvert location appears to be the most favorable location for a new culvert because:

- Shortest distance to deeper Sound waters;
- Inflection point in shore minimizes sand intrusion
- Existing culvert location (e.g. access, space)

Open Channel Inlet / Outlet: The existing culvert location is not considered favorable for an open inlet because:

- Space is too narrow for anticipated width and possible migration; and,
- The jog in the shore is an unstable place for a channel and channel armoring would be required.

An area of relatively low elevation with marsh vegetation located north of the existing culverts and residences was identified as a possible historic tidal connection to the sound (CGS 2010). Analyses of sediment diatoms indicate that this was primarily a freshwater and brackish area (EHH Consulting 2012). This location is a likely candidate for restoring an open channel connection between the sound and the lake, for the following reasons:

- The wave exposure is reduced relative to the current culvert location;
- The sand transport pathway diverges slightly offshore from the cobble berm; and,
- The northerly direction of mouth migration is more predictable, and there is little damage risk due to the lack of infrastructure in this location.

2. Wave Climate and Sediment Transport

The geomorphology along the shore at Swan Lake is highly dependent on the wave climate incident to the site. The site is exposed to locally generated wind waves and swell propagating through the Strait of Juan de Fuca from the Pacific Ocean. Low amplitude waves with a period of approximately 15 seconds were observed during a site visit on May 14, 2012. Also, wave heights and directions for swell and wind waves are strongly affected by offshore bathymetry, and hence wave power and sediment transport rates vary with location. A 2-dimensional (2D) wave model can help establish a more complete understanding of the wave refraction effects on the nearshore wave climate incident to Swan Lake.

The following sub-sections describe wave modeling efforts using the SWAN (Simulating WAVes Nearshore) model (Delft 2011) for swell and wind waves, and the subsequent calculations of longshore sediment transport rates at the proposed northern inlet site.

2.1. Offshore Bathymetry

A nested model for SWAN was developed using offshore bathymetry data for the Salish Sea and nearshore bathymetry in the vicinity of the site. The offshore bathymetry data set for the larger grid, covering a majority of the Salish Sea, was obtained from the National Oceanic and Atmospheric Administration (NOAA) National Geophysical Data Center (Lim et al. 2011). Nearshore bathymetry was collected by CGS in May 2012, and tied into a digital terrain model (DTM) based on additional topographic data, including site surveys and LiDAR data.

The offshore bathymetry in the Salish Sea is highly irregular, with maximum depths between 100 and 300 meters and several relatively shallow shoals approximately 10 meters deep distributed throughout the basin (Figure 3). Swan Lake is also located in the shadow of Smith Island, a small island located approximately 5 miles to the west of Swan Lake.

2.2. Swell Waves

Synthetic time series of wave height, periods, and directions of swell waves incident to the site were estimated by applying spectral refraction coefficients for Swan Lake to spectral wave data collected at the New Dungeness Buoy (NDBC 46088). The refraction coefficients are used to predict the nearshore wave characteristics resulting from focusing and spreading induced by relatively shallow sea bed forms along the wave travel paths. A series of SWAN model simulations were conducted with unit wave height under different wave direction (θ) and wave period (T_p) combinations, varying from 265° to 275° and 10s to 22s, respectively. Refraction coefficients were calculated as the ratio of refracted wave heights in 6 meters depth offshore of Swan Lake to the incident wave height at the New Dungeness Buoy (Figures 4 and 5). For this analysis, we assumed that the boundary condition wave height was representative of the wave heights at the New Dungeness buoy. The values of the refraction coefficients for five locations off of Swan Lake varied from 0.3 to 0.8 (Table 2). Values of the refraction coefficients did not vary significantly with changes in the incident deepwater wave angle, and so the values reported in the table represent averages over incident wave direction. The refraction coefficients reported in this memorandum represent wave height ratios, as opposed to ratios of spectral energy.

Table 2. Refraction coefficients for swell waves as a function of spectral frequency (wave period) bin.

Site	$T_p=10s$	$T_p=14s$	$T_p=18s$	$T_p=22s$
Ref 1	0.5	0.5	0.4	0.4
North Inlet	0.5	0.4	0.4	0.3
Ref 2	0.5	0.4	0.4	0.3
Existing Culvert	0.5	0.4	0.3	0.3
Ref 3	0.6	0.4	0.3	0.3
Ref 4	0.8	0.6	0.5	0.4

The refraction coefficients for Swan Lake North Inlet site were applied to the spectral data (hourly measurements from 2004 to 2012) obtained from the New Dungeness buoy yielding a synthetic time series of wave heights, periods, and directions at the site. Figure 6 shows a comparison of the wave heights calculated from the spectral energy at the New Dungeness buoy (blue) and at Swan Lake North Inlet (red). The peak wave period for the transformed waves was selected from the frequency bin that contained the maximum amount of spectral energy. The nearshore wave directions for waves at the North Inlet location were identified based on the transformed peak period, and range from 287° to 297° . These directions are presented in Table 3.

Table 3. Nearshore wave directions after transformation from offshore.

Site	$T_p=10s$	$T_p=14s$	$T_p=18s$	$T_p=22s$
Ref 1	284	291	295	290
North Inlet	287	294	297	297
Ref 2	287	293	296	296
Existing Culvert	285	293	296	296
Ref 3	279	289	295	296
Ref 4	279	283	285	285

The results of the swell modeling indicate that the offshore bathymetry plays an important role in the refraction from offshore to nearshore, and effectively reduces the wave heights overall. Incident waves are dissipated by Smith Island, with reduced wave energy incident to the site relative to the New Dungeness buoy. In contrast, the shoals located to the West and South of Smith Island focus wave energy generally in their lee while inducing reduced wave energy elsewhere. It should be noted that “unit” wave heights (one meter) were used as a basis to

develop wave height transformation ratios and Smith Island was not modeled as a complete barrier but as a highly dissipative area that effectively acts as a barrier in the model. Also, the long period waves are more affected by the offshore bathymetry than shorter period ($T_p < 14s$) waves, owing to their longer wavelengths. This suggests that mid-period swell contributes a bulk of the amount of energy to the site at Swan Lake, whereas longer period energy contributes less. A maximum wave height of 3.8 feet was estimated for the transformed waves at Swan Lake, compared to maximum wave height of 9.7 feet observed at the New Dungeness buoy, although the average wave height for both time series was less than one foot.

A more detailed analysis of waves could be accomplished by modeling the entire Strait of Jaun de Fuca, out to deep water in the Pacific Ocean. However, such an effort would increase the computational requirements significantly. Also, other models that include wave diffraction may provide more accurate results for the lee of Smith Island. If additional work on wave exposure is applied, we recommend installation of one or more wave recorders nearshore to directly measure the waves, and evaluate whether an adequate empirical relationship can be developed without additional modeling, and to inform any future modeling that may be desired.

2.3. Wind Waves

The wind wave climate at the site was characterized using wind data and wind wave hindcasting. Wind data in a percent occurrence basis from the Smith Island wind gage were used (NDBC Station SISW1). Approximately 28 years of hourly 2-minute average wind speed measurements were used to develop a wind rose, indicating the percent time that a particular wind magnitude occurs from a given duration (Figure 7). As shown in the figure, the predominant wind directions are from the west and southeast, with the greatest magnitude generally associated with winds blowing from the southeast. The SWAN model was used to simulate wind waves with a constant wind field for a range of wind directions varying by 10° from 160° to 360° , which is the range of wind wave directions incident to the site. The SWAN model used for the swell propagation was also used for the wind wave hindcasting. The steady state version of SWAN predicts wind wave generation as a fetch-limited condition for a given windspeed without checking whether the wave growth is duration-limited. A wind speed duration of 3-hours was selected that would approximately yield a fetch-limited solution for the range of fetches offshore of the site. The algorithm used to relate wind speed and duration is that described in the Shore Protection Manual (USACE 1984).

The wave height, period and direction output from the SWAN model for the different wind speeds and directions were multiplied by the fraction of occurrence (also called percent occurrence) for the particular wind speed and direction, resulting in wind wave height and period roses (Figure 8). The wind wave modeling results indicate maximum wave heights and periods of approximately 5.5 feet and 5.5 seconds, respectively, but the predominant condition is a wave with height less than 2 feet and period less than 3.5 seconds. The predominant wind wave direction is from the west-southwest (approximately 260°), although periods of relatively high wave power are incident to the site from the west and the west-northwest.

2.4. Annual Wave Power

Wave power from both swell and wind waves was estimated incident to the site. Wave power derived using linear (small amplitude) wave theory can be described by the equation

$$P = \frac{\rho g H^2 T}{32\pi} \quad (1)$$

where P is wave power (ft-lbf/sec/ft of crest length), γ is the unit weight of sea water (64.1 lbf/ft³), g is the acceleration of gravity (32.2 ft/s²), H is the root-mean-square (rms) wave height (ft), and T is wave period (sec). This equation can be reduced to $P=20.5H^2T$ by combining the constants.

The average power per year for swell at the Northern Inlet site was estimated by integrating the wave power time series and dividing by the number of years of the record. The procedure yielded an average power per year of 2.2×10^9 ft-lbf/ft-yr that is contributed by swell.

The total power per year for wind waves at the Northern Inlet site was estimated by computing wave powers for each particular combination of wave height, wave period, and incident direction, and weighting by the percent occurrence for that particular combination. Within a particular direction bin the total power per year is the potential wave power (Equation 1) multiplied by the percentage of time that a wave with a given height and period occurs, and finally by the number of seconds in a year (see bottom panel of Figure 8). Summing up over all directions resulted in a total power per year of 0.4×10^9 ft-lbf/ft-yr that is contributed by wind waves.

Assuming that the swell and wind wave power are independent, the total combined wave power per year can be estimated by adding the swell and wind wave contributions together. This yields a combined wave power per year of 2.6×10^9 ft-lbf/ft-yr at the Northern Inlet site. The wave power at the location of the existing culverts was not calculated, but is likely very similar to the estimates for the Northern Inlet site because the values of the wave refraction coefficients are almost the same. This is comparable to sites with similar exposure to wind waves and swell, such as Crissy Field in San Francisco Bay, for which the total power per year was estimated to be approximately 1.8×10^9 ft-lbf/ft-yr, and was approximately verified with measurements of sand accretion (Battalio et al. 2007).

2.5. Longshore Sediment Transport

Wave induced longshore sediment transport, or longshore drift, was estimated using two different methods. The first method used was the deepwater version of the Coastal Engineering Research Center (CERC) formula (USACE 1984). This method was used to estimate the potential sediment transport rate, and would likely represent an overestimation in supply-limited conditions. However, it is an indication of the total potential of transporting sand that could occur. A drawback of this method is its questionable validity for the application to large sediment, such as cobble that is found at project location. The second method used was the Kamphuis (1991) method, which accounts for sediment size. This equation was applied to both sand and cobble sized particles that were observed. The following describes the application and results of these methods.

The CERC formula methodology is described by the equations

$$Q(\text{cy} / \text{yr}) = 7500 \left(\frac{\text{cy} - s}{\text{lb} - \text{yr}} \right) P_{ls} \left(\frac{\text{ft} - \text{lb}}{\text{ft} - s} \right) \quad (2)$$

and,

$$P_{ls} = 0.05 \rho g^{3/2} H_{so}^{5/2} (\cos \alpha_o)^{1/4} \sin 2\alpha_o \quad (3)$$

where Q is the annual potential sediment transport rate (cy/yr), P_{ls} is the longshore energy flux factor (ft-lb/ft-s), ρ is the fluid density of sea water (1.99 slugs/ft³), g is the acceleration of gravity (32.2 ft/s²), H_{so} is the significant deepwater wave height (ft), and α_o is the deepwater incident wave angle. The CERC formula contains a

calibration constant, K , which is typically calibrated at the field site for best accuracy (pre-set for typical sand conditions within the constant of “7,500” in Equation 2). This parameter is intended to account for sources of variability that are not explicitly included in the prediction, such as sediment grain size. The standard accepted value for sandy beaches is $K=0.39$, but more recent work on gravel beaches has shown that an appropriate value is much smaller ($K = 0.05$), to account for the smaller transport rate for relatively heavier sediment (Alegria-Arzaburu and Masselink 2010). To our knowledge, there is no generally accepted value for sediments larger than gravel.

The deepwater CERC formula was applied to the nearshore swell wave heights estimated for the Northern Inlet site. Here, a shore angle of 315° was assumed. The resulting wave angles incident to the shoreline therefore ranged from 30° to 19° for the shorter and longer period swell, respectively. A time series of Q was calculated based on the given parameters, and then averaged to yield the net annual sediment transport rate for sand of 48,100 cy/yr to the north for swell, and 50,100 cy/yr to the north for wind waves. Due to the southward components of wind waves, as shown in the wind wave roses in Figure 8, the southward potential sediment transport was calculated to be 2,300 cy/yr. A summary of the potential sediment transport is provided in Table 4, along with the results for coarser sediment. Although no calibration coefficient exists for cobble, the results suggest that cobble transport rates would likely be less than 10,000 cubic yards per year. Although the wind waves provide significantly less power than the swell waves, they contribute an approximately equal amount of longshore sediment transport potential which is likely because the angle of incidence of wind waves is predominantly greater than for the swell.

Table 4. Potential sediment transport rates for the North Inlet site based on the deepwater CERC formula.

Sediment Transport Rate (cy/yr)	Swell Waves	Wind Waves	Total Combined
Calibration for sand ($K=0.39$) ¹			
Q_{Net}	48,100	50,100	98,200
Q_{Gross}	48,100	54,700	102,800
Q_{North}	48,100	52,400	100,500
Q_{South}	0	2,300	2,300
Calibration for gravel ($K=0.05$) ²			
Q_{Net}	6,170	6,910	13,080
Q_{Gross}	6,170	7,210	13,380
Q_{North}	6,170	7,060	13,230
Q_{South}	0	150	150

¹USACE (1984)

Alegria-Arzaburu and Masselink (2010)

Longshore drift was also estimated using the Kamphuis (1991) method to account for sediment size. The relation has the following form:

$$Q_u = 2.27 H_{sb}^2 T_p^{1.5} m_b^{0.75} d_{50}^{-0.25} \sin^{0.6}(2\theta_b) \quad (4)$$

where Q_u is the transport rate of underwater sediment, H_{sb} is the breaking wave height, T_p is the peak wave period, m_b is the beach slope from the breaker line to the shoreline, d_{50} is the median sediment grain size and θ_b is the breaking wave angle in relation to the shore-normal direction. This is converted to the total immersed volume transport rate by accounting for typical beach porosity and sediment density:

$$Q = \frac{Q_u}{(\rho_s - \rho)g(1 - \lambda)} \quad (5)$$

where ρ_s and ρ are the sediment and water densities, respectively, g is the gravitational acceleration constant and λ is the porosity of the sediment (taken as 0.4). H_{sb} was estimated from the nearshore model output of H_s using a relation provided by Komar (1998). The beach slope was estimated from measured transects of offshore bathymetry north of the lake. Representative values of d_{50} were used to assess the transport rate of sand (0.5 mm) and coarser sediments (50 mm) from the site. A shore-normal of 315° was used, generally giving incident wave angles less than 30° .

Annual average longshore drift rates were lower for Equations 4 and 5 than for the CERC formula (Equations 2 and 3). Values of 22,350 cy/yr and 7,470 cy/yr were found for sand and cobble, respectively, using the Kamphuis method (Equations 4 and 5). This should be considered as an upper bound of cobble transport, as the limited available research suggests that the majority of the transport occurs on the beach face, rather than in the alongshore current (Mason and Coates 2001). For sand, the method of Kamphuis (1991) typically provides lower values than those of the more widely-used CERC formula, but these have been shown to have lower uncertainty, since this method accounts for factors that influence breaker type, which are known to be important for longshore sediment transport (Smith et al. 2004). However, this method has also been shown to systematically underpredict the transport of larger sediments (Alegria-Arzaburu and Masselink 2010).

Considering both the CERC and Kamphuis estimates, the net annual drift of sand is likely no greater than ~100,000 cubic yards per year, while the transport of cobble is much lower, likely between 5,000 and 10,000 cubic yards per year. Since the latter was estimated using a representative cobble size of 50 mm (~2 in.), transport of the largest sediment grains present (5-9 in. cobble) would probably be less than 5,000 cubic yards per year.

3. Inlet Analysis for Swan Lake

3.1. Inlet Stability and Sustainability

Inlet stability varies widely among small lagoon systems. An inlet may have a stable cross section and occupy a fixed location, or it may migrate and close intermittently. Stable (permanently open) inlets maintain a balance between wave-driven processes that tend to close the channel and tide-driven processes that tend to scour it. For systems with an imbalance of sediment imports and exports, inlet stability is often parameterized as a ratio of terms that represent these opposing processes. Wave power and alongshore sediment drift rates usually characterize the sediment inputs while tide power or the tidal prism (intertidal volume) is used to assess the scouring influence of tides (Bruun & Gerritsen 1959; O'Brien 1971).

A perched overflow state is also a possible outcome, which does not fit within the definition of either closed or open inlets. Although under-reported in the literature, perched overflow lagoons are widespread (Cooper 2001; Perissinotto et al. 2010), and are generally characterized by a lagoon with mean water elevations well above mean sea levels, often with a one-way supratidal spill channel draining the lagoon (Perissinotto et al. 2010). Currents in these systems are insufficient to erode the channel bed to low tide levels (and thus reintroduce tides), but in stably perched systems, the bed elevation is too high to allow enough wave deposition to cause full channel blockage. This state is common for systems with small tidal prisms, such as Gulf Road Lagoon, located in Whatcom County north of Bellingham at the southeast end of the Strait of Georgia with a fetch and swell exposure similar to Swan Lake (CGS 2011). Research has also shown that it does not preclude fish passage, especially if the channel thalweg is below MHHW tide levels (Perissinotto et al. 2010).

It is important to note that installation of an open channel through the berm at Swan Lake would increase high water levels inside the lagoon as compared to existing conditions. This topic is discussed in the accompanying Hydraulic Modeling memo for this study.

A rating system can be used to classify the stability of an inlet by evaluating the ratio of neap tidal prism (small tide range during bi-monthly phases of the moon) to total annual littoral drift (Bruun and Gerritsen 1959; Bruun 1966; Bruun 1978). The neap tidal prism at Swan Lake is taken as the difference in lake storage between higher high tide and lower low tide elevations during neap tides in the adjacent sound. Using the estimated longshore drift rates for sand, the Bruun ratio varies from 5-25, indicating that tidal conveyance may be limited by buildup of sediment in the inlet. Applying this method with longshore drift rates calibrated for coarser sediment raises the ratio to 40-50, which is still within the expected range for inlets that are partially blocked by buildup of coarse sediments. The Bruun ratio indicator on its own does not predict closure, but rather indicates that the inlet, while open, may have severely limited depth and limited tidal interaction (i.e. some degree of perched behavior is expected). The Bruun stability criterion is intended as an approximate indicator only, since it is limited by the accuracy of longshore drift measurements and does not explicitly account for flows in the inlet. This method was also developed for and originally applied to inlets on sand beaches, so it is unclear whether its extrapolation to cobble provides a useful analogue. However, we suspect that the issue of inlet closure at the Swan Lake site has more to do with buildup of a cobble berm by storm waves rather than sand depositing in the inlet.

Since sediment transport rates are not always available and are highly uncertain, Johnson (1973) developed a simplified approach of comparing the estimated average annual deep water wave power with the potential diurnal (MHHW to MLLW) tidal prism. Compiling several reference lagoons that exhibit characteristics of being always open, seasonally open, or mostly closed, Johnson concluded that for a given wave power, there appears to be a tidal prism that must be exceeded if the inlet is to remain fully open to tidal interaction. A study of Bolinas Lagoon (Philip Williams & Associates (PWA) 1999; see also Battalio et al. 2007) noted corrections to the data from Johnson (1973) that affect the wave power values reported but not the validity of the approach.

Johnson's (1973) original analysis includes several coarse-sediment systems, and additional studies have also shown them to exhibit a range of stabilities (Webb et al. 1991; Walker et al. 1991). Although research on these systems is rare, there is evidence of inlets on gravel and cobble beaches in the United Kingdom (Cundy et al. 2002; Burningham and French 2006) and of cobble-armored inlets in California (Webb et al. 1991; PWA 2005). Recent work also indicates that many Puget Sound inlets reside on beaches of coarse sand and gravel (CGS 2011). We added several coarse-sediment reference sites to Johnson's original diagram to add confidence in its result.

Johnson's (1973) diagram is shown in Figure 9, which includes data from both sand beaches and sites with coarser sediment. The drawn barrier between open and closed inlets is subjective, but indicates the important result that the balance of wave and tidal power enforce a strong control on inlet behavior. Inlets with high wave power (i.e. greater sediment deposition in the inlet) relative to tidal power (i.e. flushing capability) tend to be closed most of the time. To determine how sediment size influences this relation, we present a separate chart in Figure 10, including only sites dominated or armored by sediment coarser than sand. Although the beach fronting Swan Lake has bimodal sediment composed of medium sands and small to medium cobbles, coarser sediments may dominate the inlet processes (Mason and Coates 2001; CGS 2011).

The resulting diagram indicates that the Swan Lake inlet should remain stable as compared with other systems with similar beach sediments, owing to the relatively low amount of wave power present at the site. The

interference imposed by Smith Island on swell waves arriving from Juan de Fuca Strait effectively shields much of the shoreline in the vicinity of Swan Lake. The change in orientation of the coastline from northerly to northeasterly at the current tide gate location also likely has a large impact. Swell wave energy is predicted to be higher to the south of this point, and the northerly-directed littoral drift may have a shadow to the immediate north, owing to the rapid change in shoreline position. The position of the Swan Lake site on this diagram was located with uncertainty in regards to the tidal prism. Here, we have assumed that a range in the tidal prism from a low estimate (between MTL and MHHW) and a high estimate (between MLLW and MHHW). This assumption was included because of the uncertain nature of the relationship of tidal prism and inlet dynamics and geometries for coarse cobble material. Since the boundary between stable and unstable inlets provided by Johnson is subjective, the possibility for instability (as suggested by the Bruun stability analysis) should not be neglected.

Neither the Bruun (1978) nor Johnson (1973) estimates should be taken as definitive, although they are among the most widely-used tools for assessing inlet stability. The former was intended and calibrated for inlets on sand beaches and developed primarily for large-navigable inlets, while the latter is based on a limited amount of empirical data. Both neglect many nearshore and inlet-channel processes that may also contribute to closure, such as bar-welding and the interaction between the inlet and adjacent flood and ebb shoals. Both methods suggest that the inlet may be self-sustaining, but not without periodic instability, or buildup of a cobble berm across the inlet that would severely truncate tides in the lake, enforcing a perched-overflow state, such as that seen at Gulf Rd. Lagoon (Figure 11) and other small sites.

3.2. Tidal Inlet Geometry

Hydraulic geometry relationships between the tidal prism and the cross-sectional area of the inlet channel are also common criteria applied to predict tidal inlet stability (Battalio et al. 2007). These relationships are well established for relatively large inlets and have been verified with a large amount of empirical evidence (O'Brien 1931; Jarrett 1976; Townend 2005). Although small lagoon inlets tend to exhibit equilibrium area much larger than those predicted by the established relationships, their cross section area is still strongly tied to the tidal prism (Byrne et al. 1980; Hughes 2002). Through laboratory studies, Hughes (2002) established relationships that can also apply to small inlets, relating the geometry by the equations

$$A_e = 0.65k_a (C_1 P)^{8/9} \quad (6)$$

and,

$$C_1 = \frac{W^{1/8}}{[g(S_s - 1)]^{1/2} d_e^{3/8} T} \quad (7)$$

where A_e is the cross-sectional area of the inlet below mean tidal level (MTL), k_a is an empirical coefficient (with a best fit value of 1.34), P is the effective tidal prism, W is the inlet width at MTL, g is the acceleration of gravity, S_s is the specific gravity of the sediment, d_e is the median grain size of the sediment, and T is the semi-diurnal tidal period. The term $C_1 P$ is known as the modified tidal prism.

The bimodal sediment characteristics of the beach at Swan Lake and the lack of information on previous inlet conditions at the site make it difficult to directly apply the Hughes (2002) relationship. Sediment samples on the beach suggest that medium sand with an average grain size of approximately 0.5 mm exists at the current tide gate and at sites immediately to the north and south. Otherwise, the beach composition is dominated by coarse sediment, with average grain sizes of approximately 13, 31 and 90 mm at the tide gate, north and south sites,

respectively. The limited research on tidal inlets on mixed or coarse-grained beaches suggests that inlet geometry is somewhat tied to the sediment size residing in the inlet bed (e.g. Webb et al. 1991). Since gravel and cobbles require much higher currents to displace than sand, these inlets tend to be wider and shallower than their counterparts on sand beaches. To account for the possibility of either sand, gravel or cobbles dominating the inlet characteristics we examine the equilibrium area of each.

To evaluate the equilibrium inlet dimensions within a sand substrate, we use an iterative procedure drawing on the tidal prism in the lake, the relationship derived by Hughes (2002) and regressions for inlet geometry derived from other small inlets in the literature. Data on small inlets were collected from sites in Chesapeake Bay (Byrne et al. 1980), New Zealand (Hume and Herdendorf 1992) and Puget Sound (CGS 2011), and regressions were made between the inlet cross sectional area at MTL and the width and depth, respectively. Despite the different environmental conditions among these regions, power-fits to the data provided relationships with high confidence (Figures 12 and 13). The R^2 values are 0.57 and 0.87 for the fits between the cross sectional area and the inlet width and depth, respectively.

To solve for the equilibrium cross sectional area, we first assumed a channel width and invert elevation on the beach, then calculated the tidal prism as the difference in storage between MHHW and the channel invert. The storage volume as a function of water surface elevation was developed using a triangular irregular network (TIN) of the lake bathymetry. The Hughes (2002) relationship was then used to estimate the new equilibrium area, which was in turn used to estimate new channel depths and widths from the regressions. If the new depth differed from the original, it was used to calculate a new channel invert and the procedure reiterated until a stable inlet configuration was reached.

A similar iterative procedure was used for the scenario of a gravel or cobble substrate. The existing data on inlets of this type were used to find a representative width-to-depth ratio for the inlet channel at MTL. Table 5 compares sediment grain size against inlet geometry for Puget Sound sites and several sites with coarser sediment. Although more data are needed to improve confidence, the width-to-depth ratio appears to be higher for gravel, pebble and cobble inlets, ranging from 15-90 compared against 10-25 for sites with finer sediment sizes. We evaluate the equilibrium inlet geometry with a coarse substrate of local beach sediments using the same iterative procedure as for sand, but instead using a width-to-depth ratio of 60 and the assumption that the inlet channel shape is parabolic (ESA PWA 2011) as the geometry constraints.

Table 5. Inlet geometry compared against predominant inlet bed material from Puget Sound and other sites. Puget Sound sites generally have fetch-limited wave conditions while the others listed here do not.

Local Site	Width at MTL (ft)	Depth at MTL (ft)	Width-to-depth ratio at MTL	d _s (mm)	Notes
Tolo Lagoon ¹	10.4	0.85	12.3	2.7	
Third Lagoon ¹	13.0	0.95	13.7	38.0	
Heyer Pt. ¹	40.6	1.52	26.7	2.7	
Fishermans Pt. ¹	33.0	1.52	21.8	6.3	
Talagwa ¹	29.6	2.00	14.8	2.7	
Whitney Rd. Lagoon ¹	12.5	0.95	13.2	9.5	Channel was dredged to increase tide range and has not filled in owing to limited wave exposure (ESA et al. 2011). Therefore, the ratio is artificially low
East Travis Spit ¹	23.4	1.07	21.9	12.7	
Kayak Pt. (1886) ¹	22.0	1.26	17.5	2.7	
Gulf Rd. ²	~15.0	~1.0	15	100-150	
Hancock ²	~32	~2.0	16	75-150	
Additional Sites					
San Pedro Creek ³	10-80	0.1-2	40-80	~80	Cobble armor
Los Penasquitos ⁴	70	0.75	93.3	~80	Cobble armor
San Dieguito ⁴	30	0.65	46.1	2-32	Coarse sand, gravel
Tijuana ⁴	50	1.75	18-28	2-32	Coarse sand, gravel
Pagham Harbour ⁵	100	3.25	30.8	2-32	Coarse sand, gravel
San Elijo ⁶	80-120	2-4	20-60	~80	Cobble armor

¹(CGS 2011); ²(CGS 2012); ³(PWA 2005); ⁴(Webb et al. 1991); ⁵(Cundy et al. 2002); ⁶(Boland and Elwany 1994);

The estimated inlet geometries at Swan Lake are summarized in Table 6. The equilibrium invert elevation is above MLLW for all cases, suggesting that the available tidal prism in the lagoon may be insufficient to allow full tidal communication with the adjacent Sound, a common condition for small inlets (e.g. Byrne et al. 1980). Since sand is easier to flush than the coarser sediments used here, the equilibrium inlet width, depth and cross sectional area (189 ft, 2.9 ft and 563 ft², respectively) were much larger for sand than for any other case. As the sediment size increased, all dimensions decreased, suggesting that if the inlet bed were to consist of the coarsest sediment found on the beach, the geometry would be the most constrained. For a grain size of 230 mm (9 inches), the inlet width, depth and cross sectional area were estimated as 67.8 ft, 1.13 ft and 51.6 ft² at MTL, respectively.

Table 6. Equilibrium dimensions of an inlet connecting Swan Lake to Puget Sound, assuming different bed sediment grain sizes.

d _s (mm)	A _e (ft ²)	Width (ft)	Depth (ft)	Invert elevation above MLLW (ft)	Tidal Prism (Ac-ft)
0.5	563.7	189.0	2.90	1.68	509.7
13	165.3	121.8	2.03	2.55	461.0
31	116.0	102.0	1.70	2.88	439.2
90	74.8	81.6	1.36	3.22	415.4
128	65.2	76.2	1.27	3.33	408.6
230	51.6	67.8	1.13	3.47	398.5

Estimates for the gravel and cobble cases are limited by our lack of data for comparable systems. In gravel bed fluvial systems, while stream depth is tied mainly to flow rate, the bank-full channel width is known to decrease for coarser sediments (Parker et al. 2007). The opposite appears to be true of inlets, which may reflect the

influence of waves or the fact that “bank-full” conditions have less meaning as tides consistently vary the water elevation. Choosing a smaller representative width-to-depth ratio here would have the influence of increasing the depth and tidal prism while lowering the invert elevation. However, especially for cobbles, the currents provided by tidal fluctuations are typically insufficient to erode bed sediment and these changes may be unrealistic.

The present estimates may also overestimate the inlet cross-sectional area if seepage losses in the system are significant. Since no data are present to indicate the potential levels of seepage through the permeable beach, we have assumed that all flow is confined to the inlet channel. However, gravel and cobble beaches are associated with high hydraulic conductivity (Mason and Coates 2001) owing to the greater pore space between the large sediment grains, so some degree of seepage is likely.

3.3. Scour Velocities

To account for the inherent uncertainty in each of the methods described above for inlet geometry and stability, we directly calculated the velocity required for scouring the inlet bed for different sediment sizes. For the inlet to reach a stable geometry, such as those described above, some scouring potential must be available, even with the large cobbles potentially dominating the channel hydraulics. We calculated a depth-averaged scouring velocity using a methodology provided by Julien (1998). Fully-turbulent conditions and plane-bed geometry were assumed, and friction was estimated based on sediment grain size and channel depth. This was related to the minimum shear stress required for sediment transport to arrive at the required depth-averaged velocity for erosion.

Table 5 shows the results of the scouring velocity analysis. As expected, the required velocity increases with sediment size. For shallow flows (< 2 ft depth), the required depth-averaged velocity ranges from 2.57 ft/s for 0.5 inch gravel to 7.85 ft/s for 9 inch cobble. For deeper flows, a greater depth-averaged velocity is required. For depths of roughly 3 and 6 ft, the required velocity increases to 8.8 and 9.87 ft/s, respectively. Given the prediction from the Hughes (1999) analysis suggesting an invert position well above MLLW, flows in the inlet will probably be limited to the shallow or intermediate case, as the inlet may transition to a perched outflow channel over time.

Scour potential for the proposed inlet should be evaluated by comparisons of velocity model results to the scour criteria presented in Table 7 below.

Table 7. Depth-averaged velocity (ft/s) required to scour sediment based on depth (rows) and grain size (columns)

Depth	Median Grain Size, D_{50}				
	13 mm (0.5 in.)	31 mm (1.2 in.)	90 mm (3.5 in.)	128 mm (5 in.)	230 mm (9 in.)
1.6 ft (0.5 m)	2.57	3.56	5.95	6.71	7.85
3.2 ft (1 m)	2.88	3.99	6.67	7.52	8.80
6.4 ft (2 m)	3.23	4.48	7.48	8.43	9.87

3.4 Wave Berm Building

The elevation of the cobble berm was measured at three locations near Swan Lake in spring, 2012: at the existing culvert location, the proposed inlet location, and at a reference site to the north of the proposed inlet location. The elevations are summarized in Table 8 and shown in Figure 14.

Table 8. Wave-built cobble berm crest elevations in vicinity of Swan Lake

Location	Berm Elevation (feet, NAVD)	Comments
Culvert	11 to 12 ft	Bulkheads may affect berm elevation
Inlet Alternative	11.5 ft	In lee of "point" at Culvert
Reference Sites	12 to 13 ft	Multiple sites north of the culvert

These berm elevations are conceptually an indicator of the elevation of total water level (wave runup) on an annual to 10% of the year recurrence frequency (Lorang, 2002; ESA et al. 2011). These elevations are just a few feet above MHHW (+7.2 ft NAVD approximately), which indicates that the typical total water level is not that high. Assuming that wave runup is about 1 to 1.5 times the incident wave height, and that the peak total water levels occur during Sound water levels at MHHW or above, the "characteristic" berm-forming wave heights indicated are about 2 ft to 3 ft or so. However, extreme high wave conditions of around 4 ft can be expected based on the offshore buoy data with transformation to the site (see swell section, above), which would indicate a potential for onshore cobble transport above and beyond the measured elevations. Hence, it is likely that in the absence of scour or excavation, the cobble berm elevation will rise under wave action to an elevation above the tidal frame, as it exists today.

3.5 Equilibrium

The equilibrium condition of a tidal inlet or a drainage outlet is difficult to predict. Detailed studies of marginally stable (e.g. intermittently closed and open inlets / outlets) indicate that equilibrium consists of several quasi-steady states with rapid changes between them induced by extreme values of forcing parameters such as waves, tides and runoff (Battalio et al. 2007). The importance of prior (antecedent) conditions and highly variable forcing parameters on future conditions has resulted in a time-series analysis approach to address mouth stability. Where successful, these approaches have required field data to establish existing conditions, and then have been extended to changed conditions. The available field data are not sufficient to apply this methodology at Swan Lake but consideration of time-dependent processes can enhance our judgment regarding inlet stability.

The consideration of cobble transport by tidal and discharge currents and wave action indicates that the inlet / outlet is likely to have a high thalweg controlled by a wave-built cobble-gravel berm, resulting in a sill that perches the lagoon water level. Also, an increase in the berm-sill elevation will decrease discharge scour velocities, indicating a tendency for the channel to close (Escoffier 1940). Hence, if the wave and Sound water level conditions are sufficient to transport cobble into the channel and increase the elevation above MHHW, it is unlikely that the discharge due to tidal prism and typical runoff will be sufficient to remove the cobble. It is unclear whether rainfall runoff could be sufficient to eventually re-open the mouth, or what frequency such an event would be expected to occur in the existing, highly manipulated condition of the watershed. Hence, it is expected that the natural inlet would eventually be closed by waves. However, given the low wave-driven cobble transport rate, we expect that the conditions necessary to close and open inlet would not happen frequently (e.g. less frequently than annually). In this case the "inlet" would likely take the form of an "outlet" channel, or essentially a creek mouth, with water levels perched above the tide frame.

6. Implications of Results

6.1. Waves and Alongshore Sediment Transport

Swell propagating through the Strait of Juan de Fuca toward the shore at Swan Lake is affected by offshore bathymetry, including Smith Island. The result is reduced wave exposure, especially north of the existing culvert location.

The angular incidence of wind waves and swell drive a northward sediment transport potential. The change in shore angle north of the existing culvert increases the angular incidence of waves to this area, while the wave heights are reduced due to sheltering by the “elbow” and Smith Island. The effect is to reduce the potential southerly transport, and result in nearly exclusively northward transport. The steep angle of wave approach to the northern shore implies spit-like sand bar formations and ridge-like cobble transport. A sand bar shoal observed at the site is consistent with the wave and sediment transport analysis (Figure 15).

6.2. Inlet Stability

Available information indicates that a small tidal inlet could persist at the north site if excavated. The equilibrium geometry is expected to consist of an intertidal bottom elevation around mean tide level, with a width of about 80 feet. This estimated geometry is very approximate because it is based on limited reference site data and extrapolation of methods developed for sandy sediment to cobble sediment.

The potential for the inlet to close appears to be primarily associated with the potential for waves to build the cobble berm higher, thereby reducing the tide range and progressively closing off the channel. This situation would reduce the tidal action to high tides, and the mouth would function more like an outlet channel associated with small creeks and back barrier creek estuaries.

The existing culvert location does not appear to be consistent with an open inlet/outlet because the estimated inlet width, 80 ft, is too large for the space between the houses. This concern is partly based on the likelihood of mouth migration which in this area could be induced to the north or south depending on the wave directions. The northern most location is therefore preferred for an open mouth. At the northern location, the mouth will tend to migrate northward but will likely be limited by the cobble berm and hence a shore-parallel channel between the berm crest and the sand is expected to form. During large flows the channel would likely discharge directly across the shore.

Both locations may result in sand intake and formation of a flood shoal within the Swan Lake / Lagoon. The existing culvert location is probably more susceptible owing to the greater sand supply moving in the upper shore elevations, where as the northern location sand transport is somewhat detached to lower elevations. Over time, sand moving at high flood tides will migrate into the lagoon and deposit where the velocities diminish as flow spreads into the lagoon. This flood shoal could become a hydraulic control on lagoon drainage. However, we expect that discharges sufficient to maintain the mouth across the cobble should be adequate to maintain flow through the flood shoal. Given the limited sand available, we expect it will take years to decades for the flood shoal to equilibrate. During this time frame, sand supply would be slightly reduced to the shores north of the mouth.

Overall, we expect that a natural inlet channel can be maintained with structural or mechanical measures to limit or remove, respectively, wave-driven cobble deposition.

- Excavation of the cobble would be required as often as approximately every year although it is possible that this requirement could be less frequent during calmer (wave) years. Post-construction monitoring could allow a more accurate assessment of management requirements (Battalio et al. 2007);
- A jetty to the south could conceptually enhance inlet stability and reduce or eliminate excavation requirements. This structure would conceptually deflect wave-driven transport offshore, and interrupt much of the cobble transport into the inlet. To limit downdrift (north) effects, the structure would need to be of limited extent with further study required to address desired dimensions;
- A sluiceway could be constructed, essentially resembling a culvert without a top. Such a structure would conceptually inhibit cobble deposition and enhance discharge scour, while limiting the extent of maintenance excavation. While this approach is not often applied in coastal settings, it is analogous to fish passage structures in creeks;
- An open channel would increase high water levels inside the lagoon as compared to existing conditions; this is discussed in the accompanying Hydraulic Modeling memo.

6.3. Culvert

The existing culvert location is the preferred location for a new culvert. This location provides the shortest distance to deeper water. This location also has a reduced likelihood of sand deposition that could block the culvert. Design of a culvert would require modeling to inform the size, number and placement within the tidal frame. Analysis of culvert feasibility for establishing a fish-passable connection will also be subject to meeting criteria for fish passage through culverts that is accepted by state and federal regulatory agencies. Overall, we think that a culvert design will be feasible under the conditions that the velocity requirements are met, and that the design accounts for periodic episodes of relatively high sediment transport rates of sand and cobble during storm events. Other additional considerations include the potential impacts to predominant and flood water levels in the lake, and whether self-regulating tide gates will provide functional management of the system.

References

- Alegria-Arzaburu, A., and Masselink, G., 2010, Storm Response and Beach Rotation on a Gravel Beach, Slapton Sands, U.K., *Marine Geology*, Vol. 278, pp. 77-99.
- Battalio, B., Danmeier, D., and Williams, P., 2007, Predicting Closure and Breaching Frequencies of Small Tidal Inlets – A Quantified Conceptual Model, Proceedings of the 30th International Coastal Engineering Conference, 3-8 September, 2006, San Diego, CA, USA.
- Boland, J., and Elwany, H., 1994, Sand and Cobble Removal From the Mouth of San Elijo Lagoon, Report for San Elijo Lagoon Conservancy and California Coastal Commission, 18 pp.
- Bruun, P., 1966, Tidal Inlets and Littoral Drift, Universitetsforlaget, Trondheim, Norway.
- Bruun, P., 1978, Stability of Tidal Inlets, Elsevier Scientific Publishing Company, New York, NY.
- Bruun, P., and Gerritsen, F., 1959, Natural Bypassing of Sand at Coastal Inlets, *Journal of the Waterways and Harbors Division, ASCE*, 85, pp. 401-412.
- Burningham, H. and French, J., 2006, Morphodynamic behavior of a mixed sand-gravel ebb-tidal delta: Deben estuary, Suffolk, UK, *Marine Geology*, Vol. 225, pp. 23-44.
- Byrne, R.J., Gammisch, R.A., and Thomas, G.R., 1980, Tidal Prism-Inlet Area Relations for Small Tidal Inlets, Proceedings of the 17th Coastal Engineering Conference, Sydney, Australia.
- Coastal Geologic Services (CGS), 2010, Swan Lake Restoration Preliminary Feasibility Study (Final Report), prepared for Skagit Fisheries Enhancement Group and Swan Lake Watershed Preservation Group, September 14, 2010.
- Coastal Geologic Services (CGS), 2011, Reference Data for Small Lagoons in Puget Sound, database provided to ESA PWA, February 1, 2011.
- Cooper, J.A.G., 2001, Geomorphological variability among microtidal estuaries from the wave-dominated South African coast, *Geomorphology*, Vol. 40, pp. 99-122.
- Cundy, A.B., Long, A.J., Hill, C.T., Spencer, C., and Croudace, I.W., 2002, Sedimentary response of Pagham Harbour, southern England to barrier breaching in AD 1910, *Geomorphology*, Vol. 46, pp. 163-176.
- Dean, R.G., and Dalrymple, R.A., 1984, *Water Wave Mechanics for Engineers and Scientists*, Prentice-Hall, Inc., Englewood Cliffs, NJ.
- Delft, 2011, SWAN (Simulating WAVes Nearshore): a third generation wave model, Delft University of Technology.
- EHH Consulting, 2012, Diatom Analyses for Swan Lake Core C, Whidbey, Washington, Report No. 120224, prepared for CGS, February 2012.

- ESA, ESA PWA, Anchor QEA, Coastal Geologic Services, KPFF, and Pacific Survey & Engineering, 2011, Puget Sound Nearshore Ecosystem Restoration Project (PSNERP): Strategic Restoration Conceptual Engineering – Final Design Report, prepared for the Washington Department of Fish and Wildlife and the U.S. Army Corps of Engineers, March 2011.
- ESA PWA, 2011, Kayak Point Lagoon Feasibility Study: Lagoon Stability, Sustainability, and Sizing, Technical Memorandum prepared for Coastal Geologic Services Inc., March 17, 2011.
- Escoffier, F.F., 1940, The Stability of Tidal Inlets, Shore and Beach, Vol. 8, No. 4, pp. 114-115.
- Hughes, S.A., 2002, Equilibrium Cross Sectional Area at Tidal Inlets, Journal of Coastal Research, Vol. 18, No. 1, pp. 160-174.
- Hume, T.M., and Herdendorf, C.E., 1992, Factors Controlling Tidal Inlet Characteristics on Low Drift Coasts, Journal of Coastal Research, Vol. 8, No. 2, pp. 355-375.
- Island County, 2008, West Beach Tide Gates: Pipe End Repair, Construction Drawings prepared by Island County Public Works, May 29, 2008.
- Jarrett, J.T., 1976, Tidal Prism-Inlet Area Relationships, GITI Report 3, U.S. Army Engineer Waterways Experiment Station, Vicksburg Mississippi.
- Johnson, J.W., 1973, Characteristics and Behavior of Pacific Coast Tidal Inlets, Journal of the Waterways Harbors and Coastal Engineering Division, Vol. 99, No. 3, pp. 325-339.
- Julien, P.Y., 1998, *Erosion and Sedimentation*, Cambridge University Press, 300 pp.
- Kamphuis, J.W., 1991, Alongshore sediment transport rate, Journal of Waterways, Port, Coastal and Ocean Engineering, Vol. 117, No. 6, pp. 624-641.
- Komar, P.D., 1998, *Beach Processes and Sedimentation*, Prentice-Hall, Inc., Upper Saddle River, New Jersey, 544 pp.
- Lim, E., Taylor, L.A., Eakins, B.W., Carignan, K.S., Caldwell, R.J., Grothe, P.R., and Friday, D.Z., 2011, Digital Elevation Models of Port Townsend, Washington: Procedures, Data Sources and Analysis, Prepared for the Pacific Marine Environmental Laboratory (PMEL) NOAA Center for Tsunami Research by the NOAA Geophysical Data Center (NGDC), February 7, 2011.
- Lorang, M.S., 2002, Predicting the Crest Height of a Gravel Beach, Geomorphology, No. 48, pp. 87-101.
- Mason, T., and Coates, T.T., 2001, Sediment Transport Processes on Mixed Beaches: A Review for Shoreline Management, Journal of Coastal Research, Vol. 17, No. 3, pp. 645-657.
- O'Brien, M.P., 1931, Estuary Tidal Prisms Related to Entrance Areas, Civil Engineering, Vol. 1, No. 8, pp. 738-739.

- O'Brien, M.P., 1971, Notes on Tidal Inlets on Sandy Shores, Hydraulic Engineering Laboratory, College of Engineering, University of California at Berkeley.
- Parker, G., Wilcock, P.R., Paola, C., Dietrich, W.E., and Pitlick, J., 2007, Physical Basis for Quasi-Universal Relations Describing Bankfull Hydraulic Geometry of Single-Thread Gravel Bed Rivers, *Journal of Geophysical Research*, Vol. 112, F04005. doi: 10.1029/2006JF000549.
- Perissinotto, R., Stretch, D.D., Whitfield, A.K., Adams, J.B., Forbes, A.T., and Demetriades, N.T., 2010, Ecosystem Functioning of Temporarily Open/Closed Estuaries in South Africa, In: *Estuaries: Types, Movement Patterns and Climatological Impacts*, Nova Science Publishers, Inc., pp. 1-69.
- Philip Williams & Associates (PWA), 1999, Bolinas Lagoon wave power check memorandum, PWA Project #1174, Technical memorandum prepared for the U.S. Army Corps of Engineers, August 1999.
- Philip Williams & Associates (PWA), 2005, Pacifica State Beach Topographic Survey, Technical Memorandum prepared for City of Pacifica Engineering Department, October 27, 2005.
- Smith, E.R., Ebersole, B.A., and Wang, P., 2004, Dependence of Total Longshore Sediment Transport Rates on Incident Wave Parameters and Breaker Type, ERDC/CHL CHETN IV 62, 13 pp.
- Townend, I., 2005, An Examination of Empirical Stability Relationships for UK Estuaries, *Journal of Coastal Research*, Vol. 21, No. 5, pp. 1042-1053.
- USACE, 1984, Shore Protection Manual, 4th ed., 2 Vol., US Army Engineer Waterways Experiment Station, U.S. Government Printing Office, Washington, DC.
- Walker, J.R., Everts, C.H., Schmelig, S., Demirel, V., 1991, Observations of a tidal inlet on a shingle beach, *Proceedings of Coastal Sediments*, New York, NY, USA.
- Webb, C.K., Stow, D.A., and Chang, H.H., 1991, Morphodynamics of Southern California Inlets, *Journal of Coastal Research*, Vol. 7, No. 1, pp. 167-187.

Figures

Figure 1. Location map and geographic setting of the project site

Figure 2. Site map of Swan Lake showing the location of the existing culvert and proposed Northern Inlet site

Figure 3. Bathymetry of Salish Sea large grid (top) and Swan Lake nearshore (bottom) shown as depth in meters

Figure 4. Swell refraction model results from SWAN large grid for wave periods 10s to 22s – significant wave height is shown in meters

Figure 5. Swell refraction model results from SWAN nested grid for wave periods 10s to 22s – significant wave height is shown in meters

Figure 6. Significant wave height in feet shown for swell measurements at the New Dungeness buoy and for transformed swell incident to Swan Lake

Figure 7. Wind rose for Smith Island, offshore of Swan Lake

Figure 8. Wave height, period, and power roses for wind waves incident to Swan Lake

Figure 9. Modified Johnson diagram for open and closed tidal inlets as a function of annual wave power and tidal prism

Figure 10. Johnson Diagram including only sites armored or dominated by sediment coarser than sand

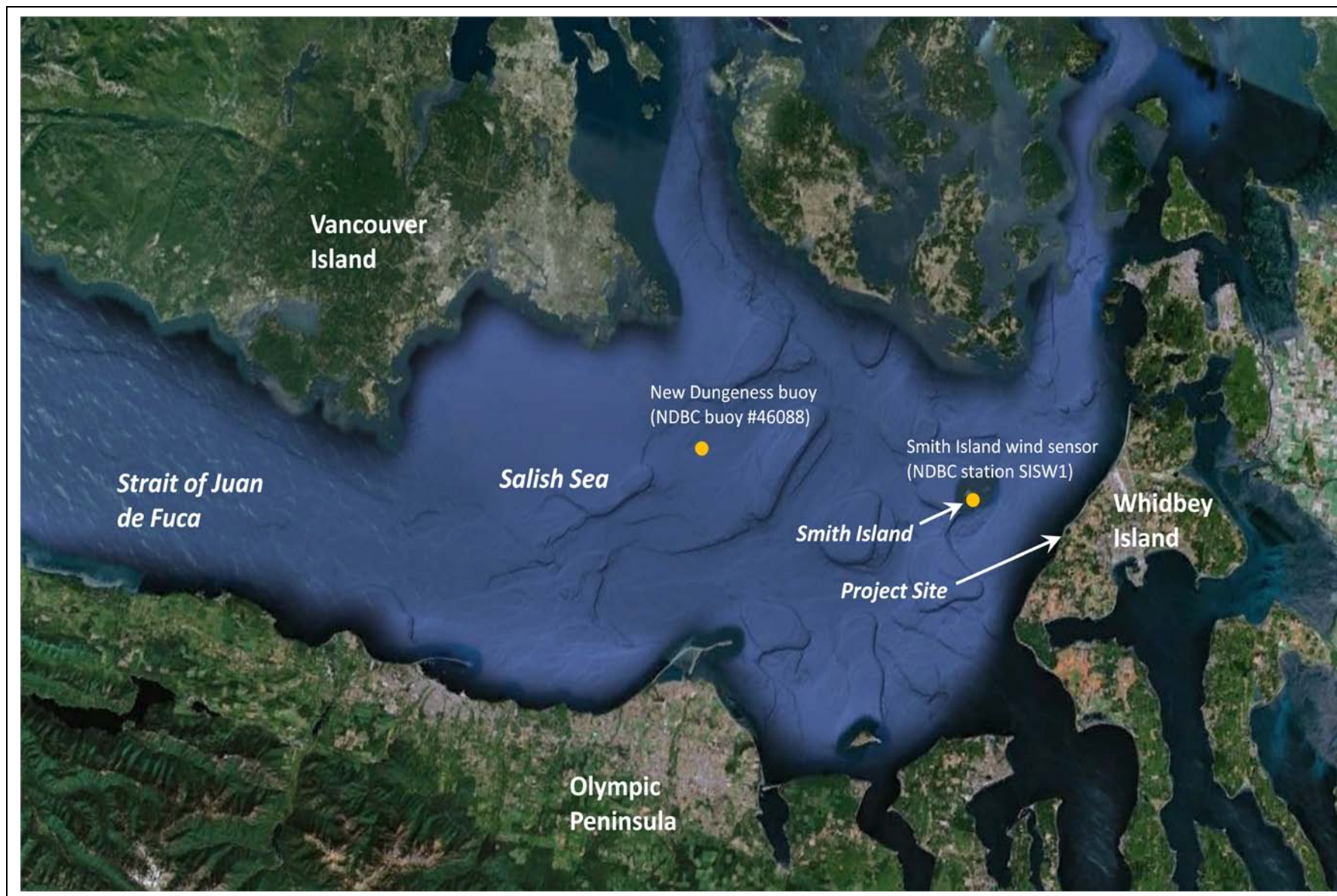
Figure 11. Geographic location and aerial view of Gulf Rd. Lagoon

Figure 12. Inlet cross-sectional area vs. inlet depth and width for small sites

Figure 13. Inlet cross-sectional area vs. inlet width and depth for all sites

Figure 14. Surveyed beach profiles – top panel shows southern sections, bottom panel shows northern sections

Figure 15. Photograph of Swan Lake shore looking north – note the sand shoal separated from the predominantly cobble beach



SOURCE: Google Earth

Swan Lake Engineering Feasibility . 120062.00

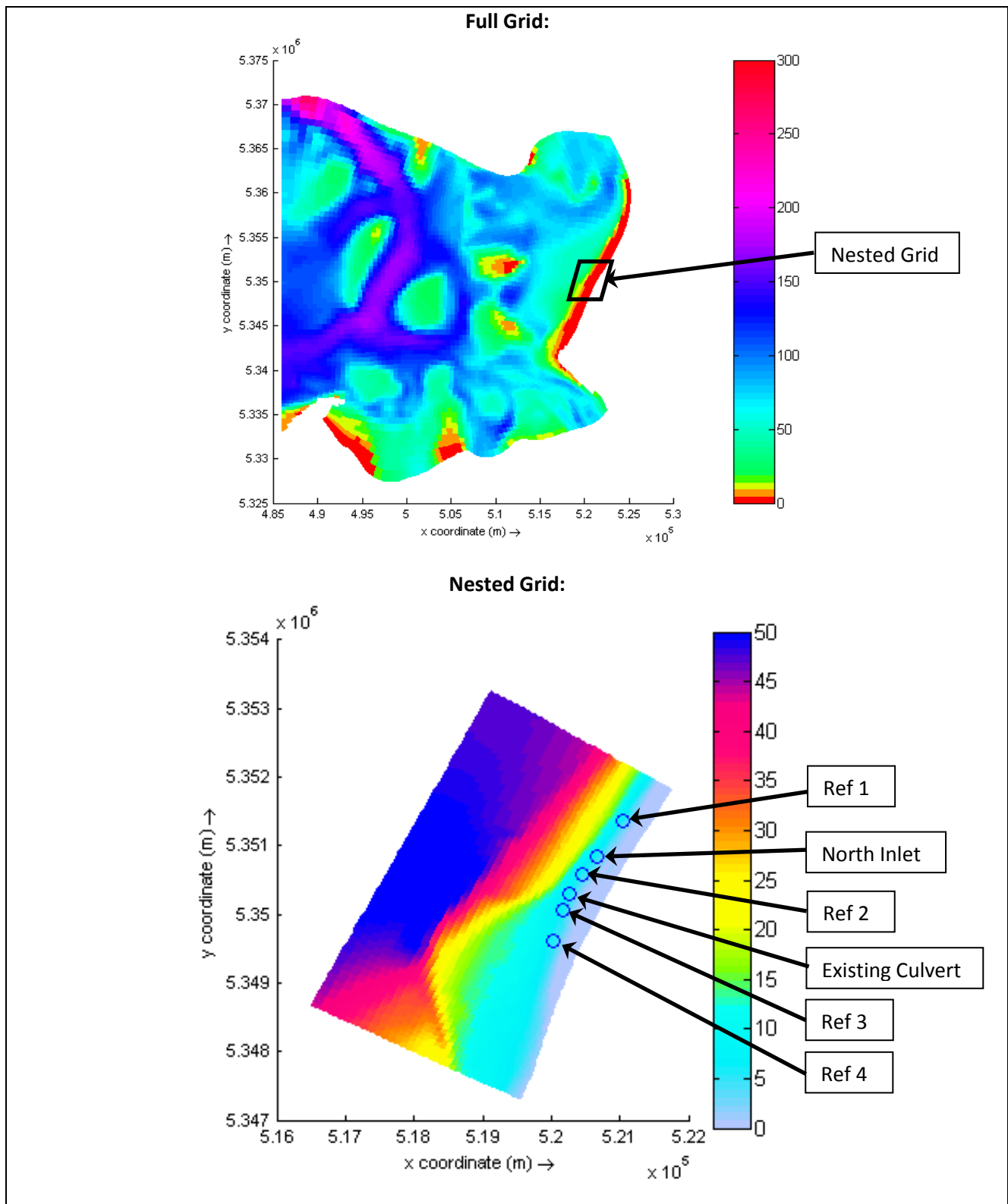
Figure 1
Location Map and geographic setting of the project site



SOURCE: Image from Google Earth

Swan Lake Engineering Feasibility . 120062.00

Figure 2
Site Map of Swan Lake showing the location of the
existing culvert and proposed Northern Inlet site



SOURCE: Lim et al. (2011) and CGS bathymetry measurements

Figure 3
Bathymetry of Salish Sea large grid (top) and
Swan Lake nearshore (bottom) shown as depth in
meters

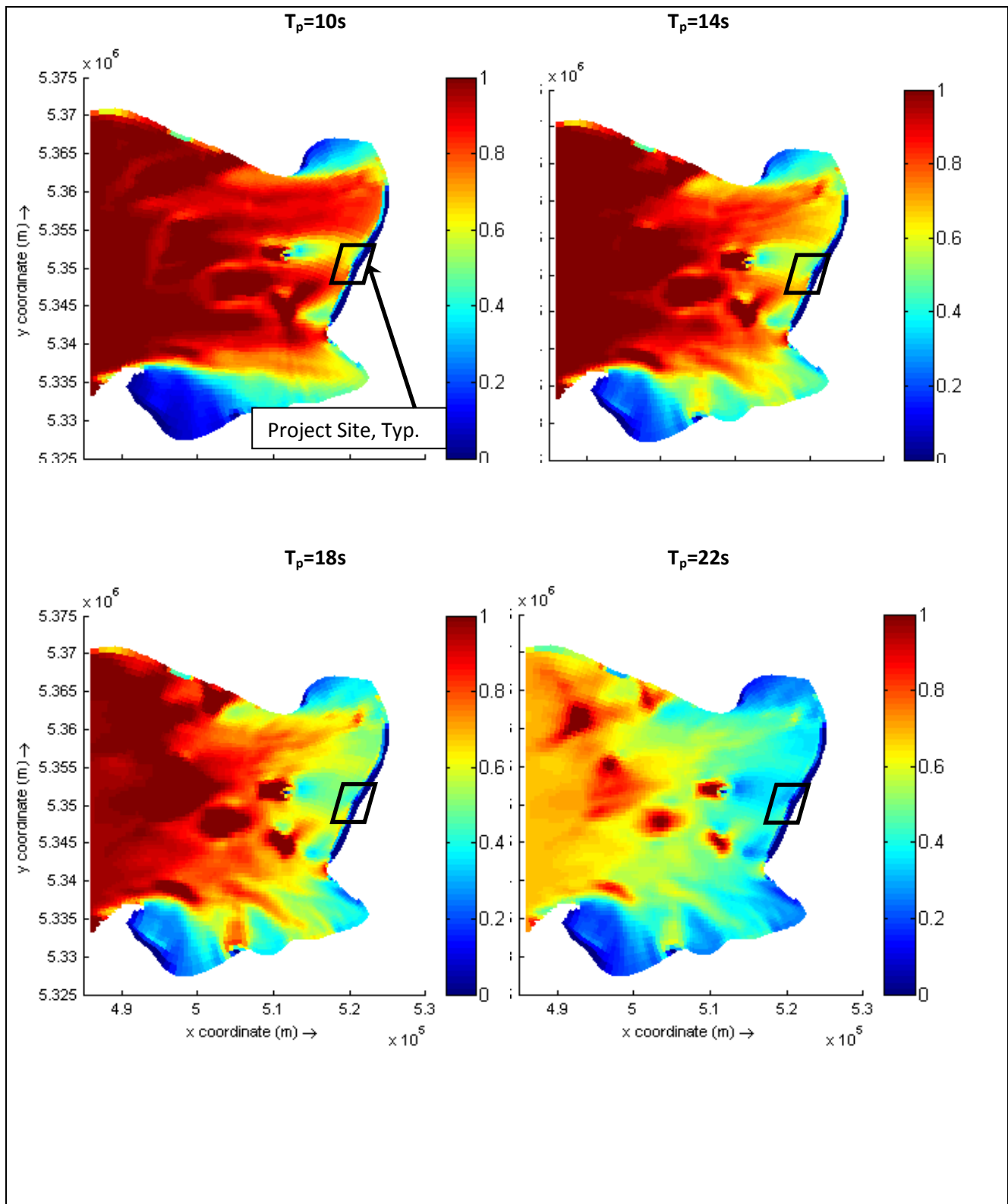


Figure 4

Swell refraction model results from SWAN large grid for wave periods 10s to 22s – significant wave height is shown in meters

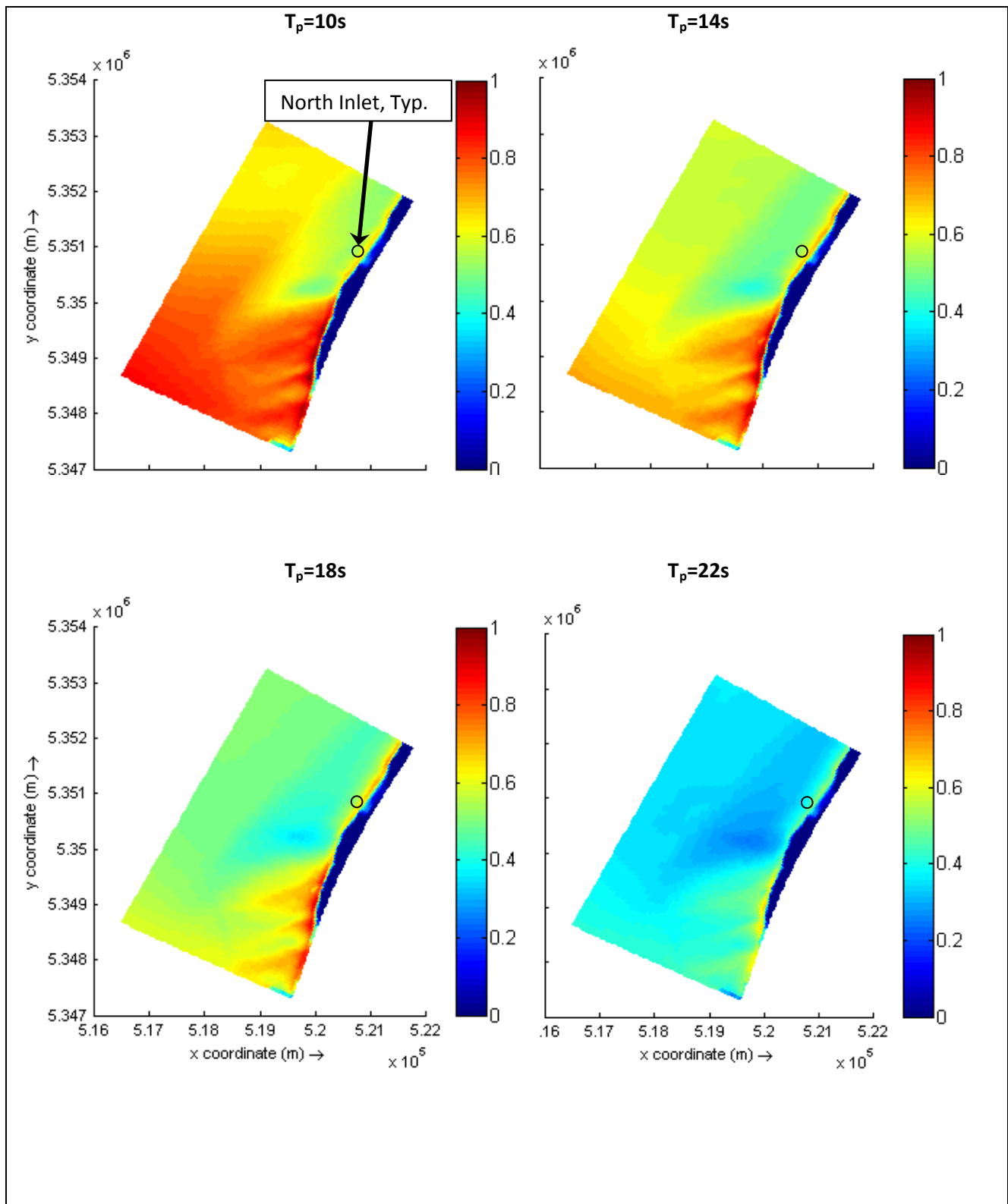


Figure 5

Swell refraction model results from SWAN nested grid for wave periods 10s to 22s – significant wave height is shown in meters

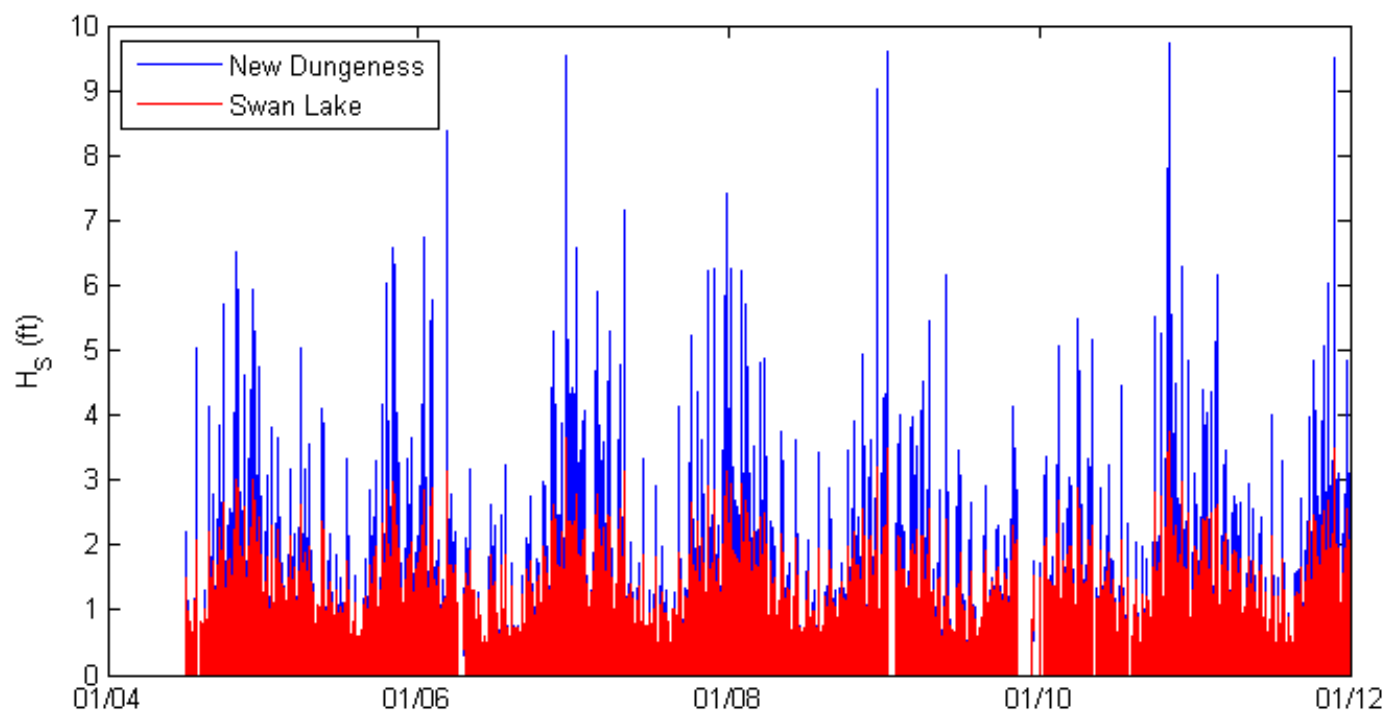
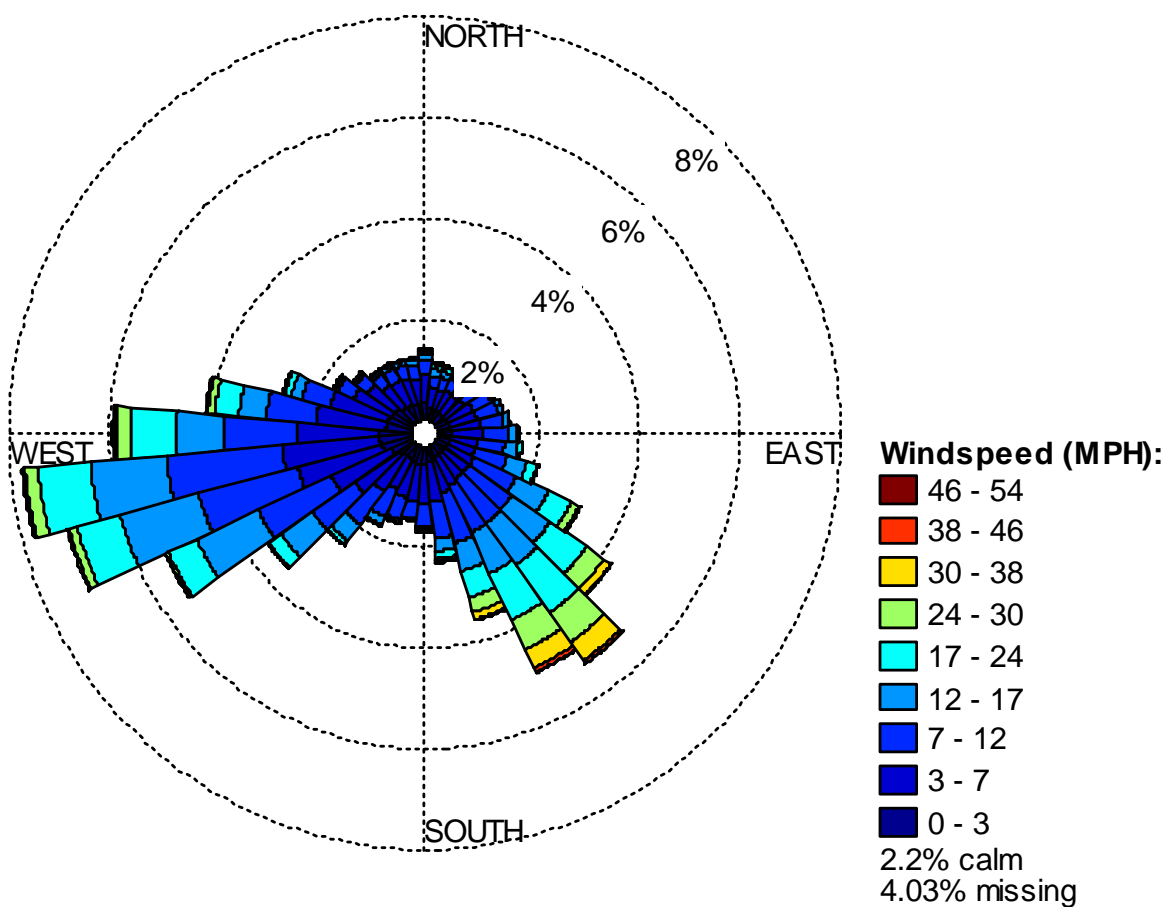


Figure 6
Significant wave height in feet shown for swell measurements at
the New Dungeness buoy and for transformed swell incident to
Swan Lake



SOURCE: NDBC Station SISW1

NOTES: Wind speeds are presented as hourly 2-min averages
Period of record is 1/1/84 – 12/31/11

Swan Lake Engineering Feasibility . 120062.00

Figure 7

Wind rose for Smith Island, offshore of Swan Lake

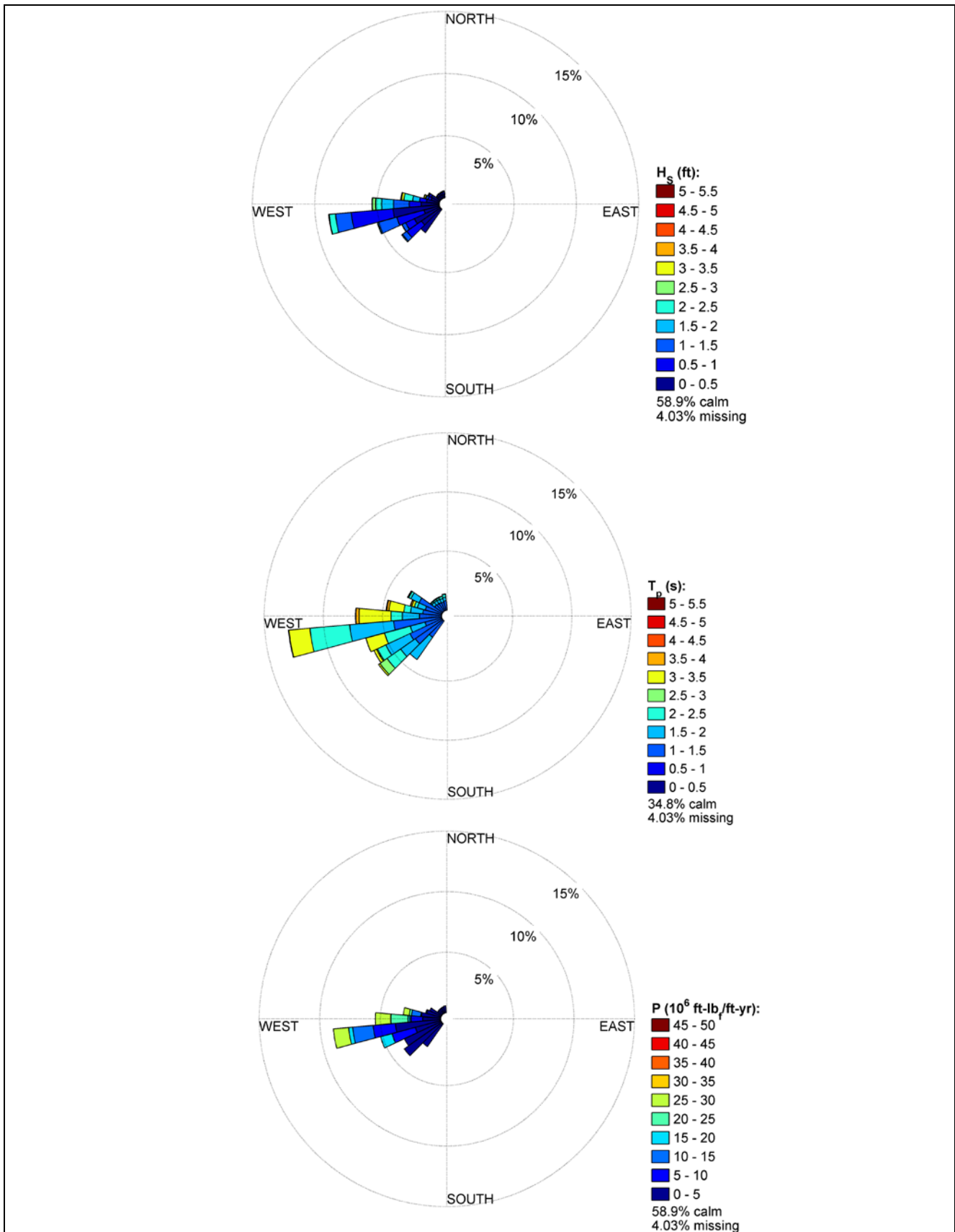
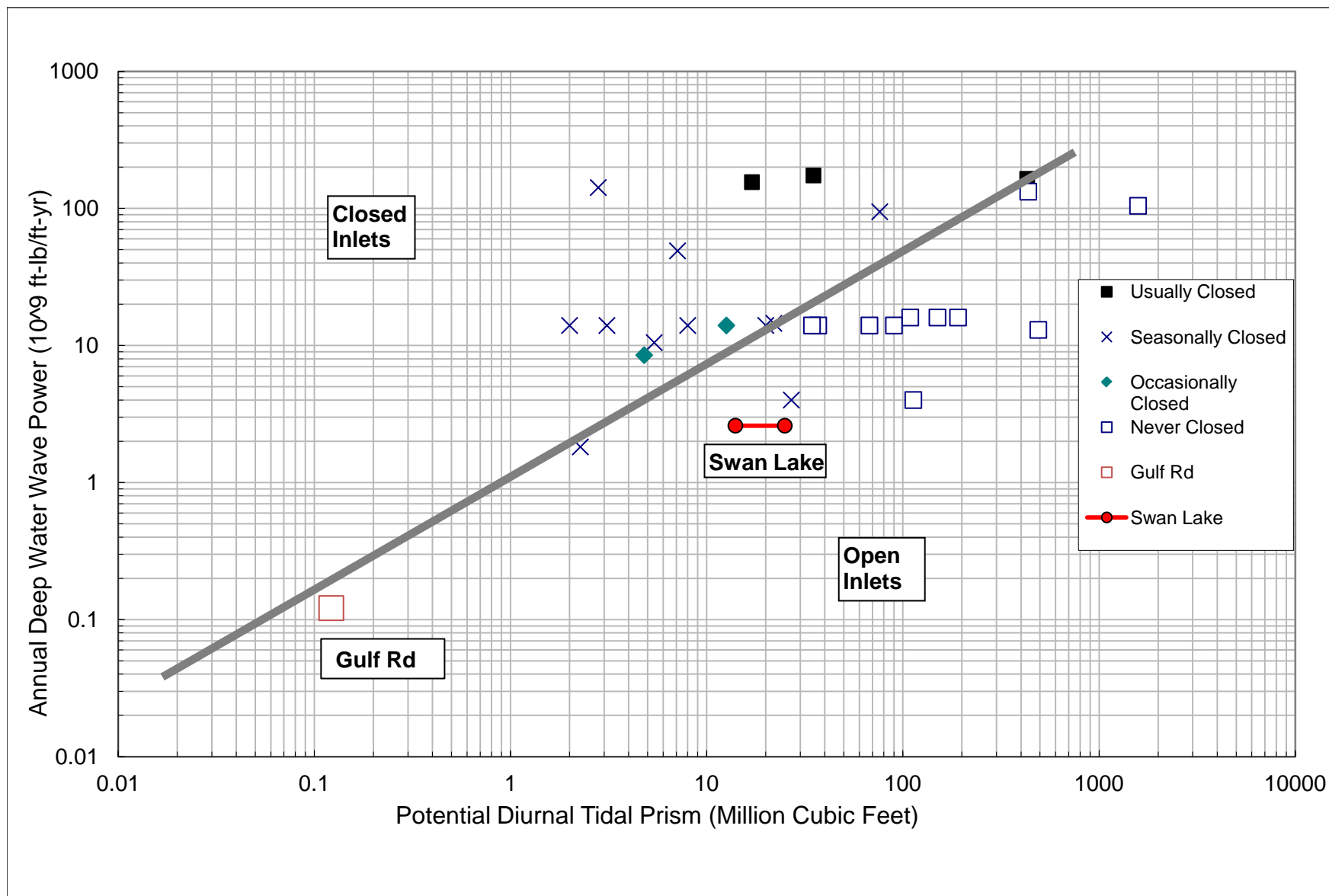


Figure 8
Wave height, period, and power roses for
wind waves incident to Swan Lake

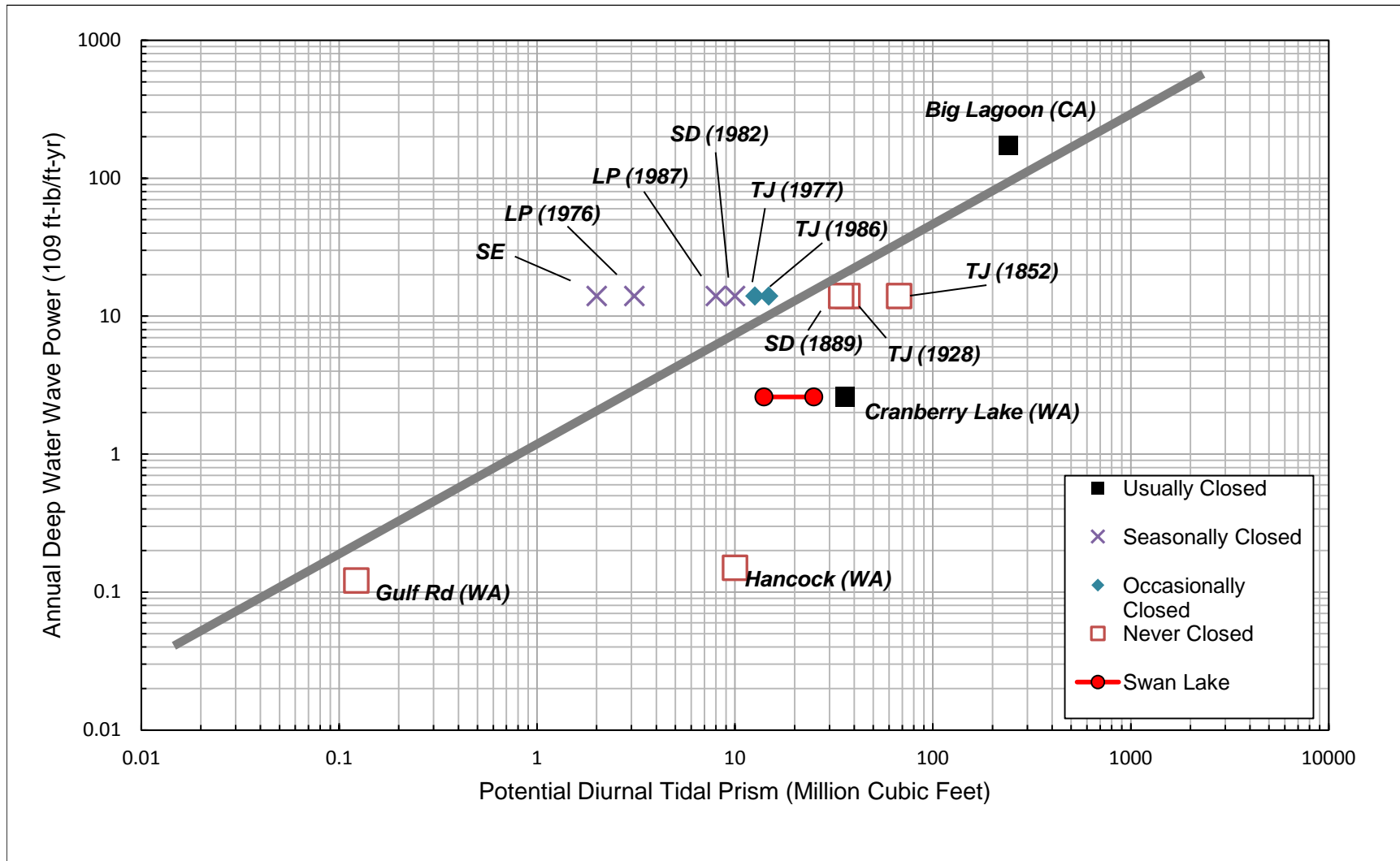


SOURCE: Original methodology developed by Johnson (1973)
Reference data compiled by ESA PWA and Coastal Geologic Services (2011)

Swan Lake Engineering Feasibility . 120062.00

Figure 9

Modified Johnson diagram for open and closed tidal inlets as a function of annual wave power and tidal prism



NOTES: Acronyms: SD=San Dieguito (CA), SE=San Elijo (CA), LP=Los Peñasquitos (CA), TJ=Tijuana (CA), CA=California, WA=Washington

Cranberry Lake is kept closed by roadway structure. Gulf Rd Lagoon and all CA sites except for Big Lagoon known to have perched overflow conditions for extended periods of time

Swan Lake Engineering Feasibility. D120062.00

Figure 10

Johnson Diagram including only sites armored or dominated by sediment coarser than sand

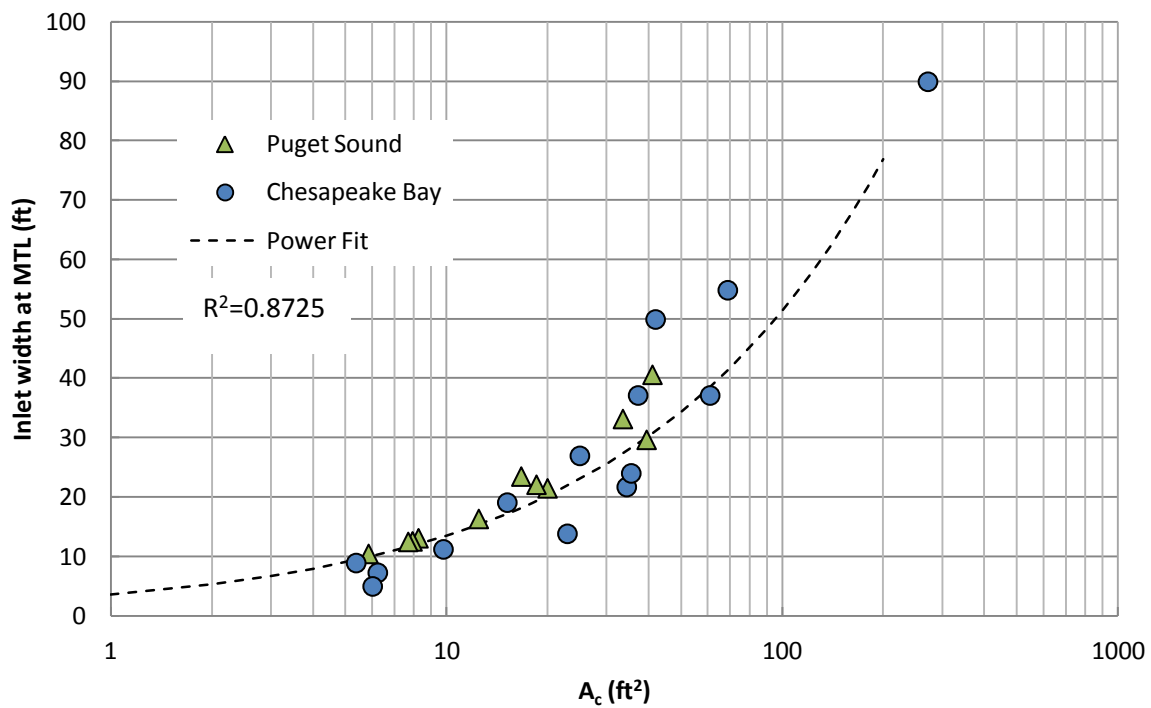
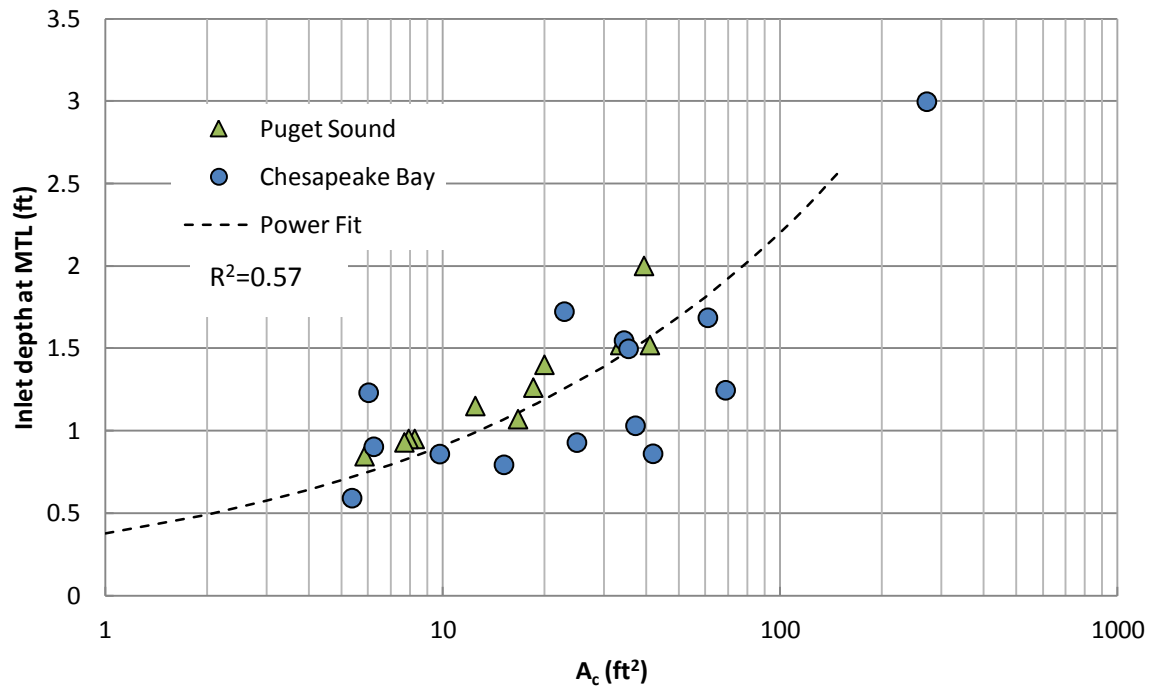


SOURCE: Bing Maps © Microsoft 2012

Swan Lake Engineering Feasibility . 120062.00

Figure 11

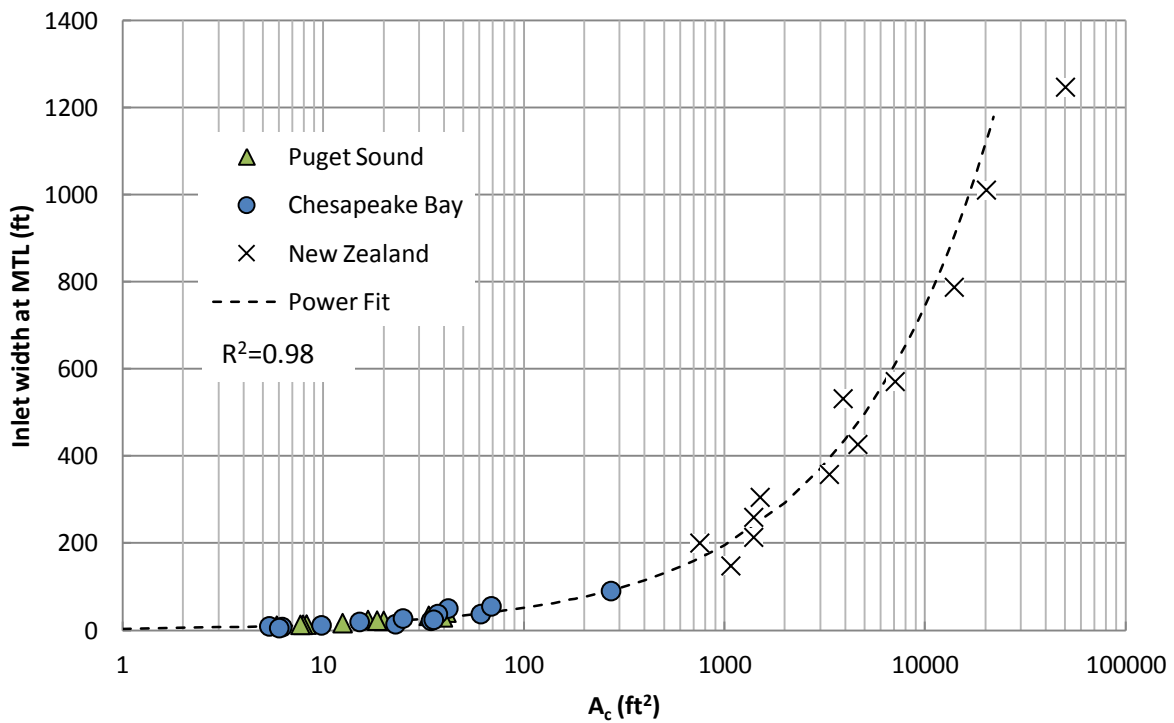
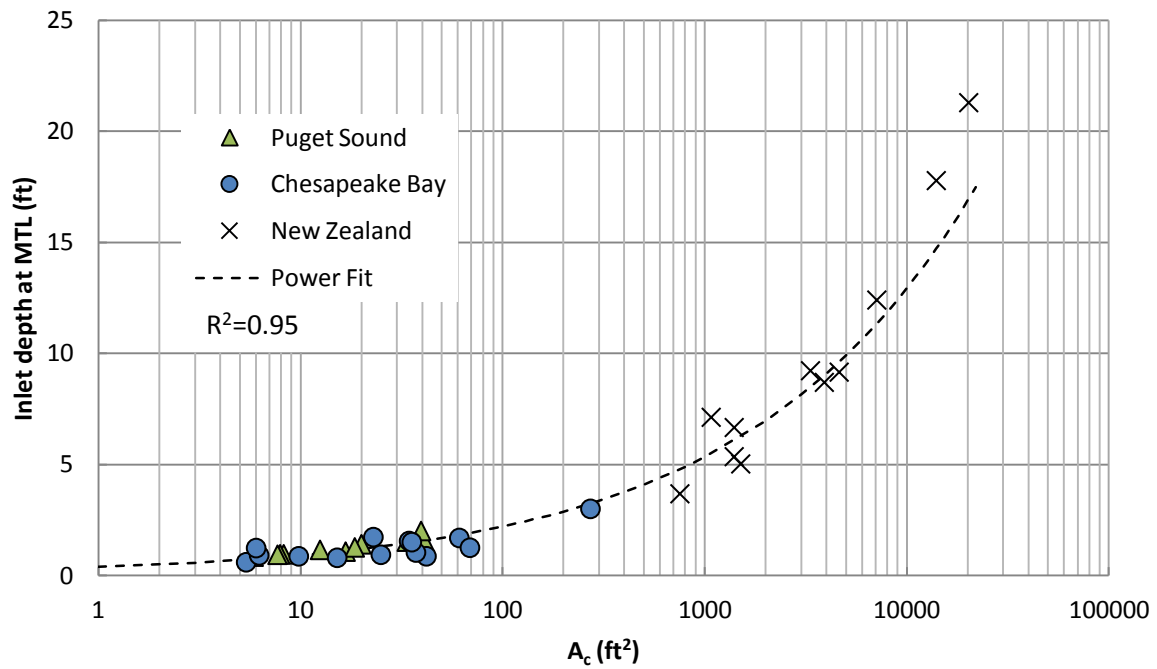
Geographical location and aerial view of Gulf Rd.
Lagoon



SOURCE: Puget Sound (CGS, PWA, 2010) and inlets from Chesapeake Bay (Byrne et al., 1980)

Swan Lake Engineering Feasibility . 120062.00

Figure 12
Inlet cross-sectional area vs inlet depth and width for small sites

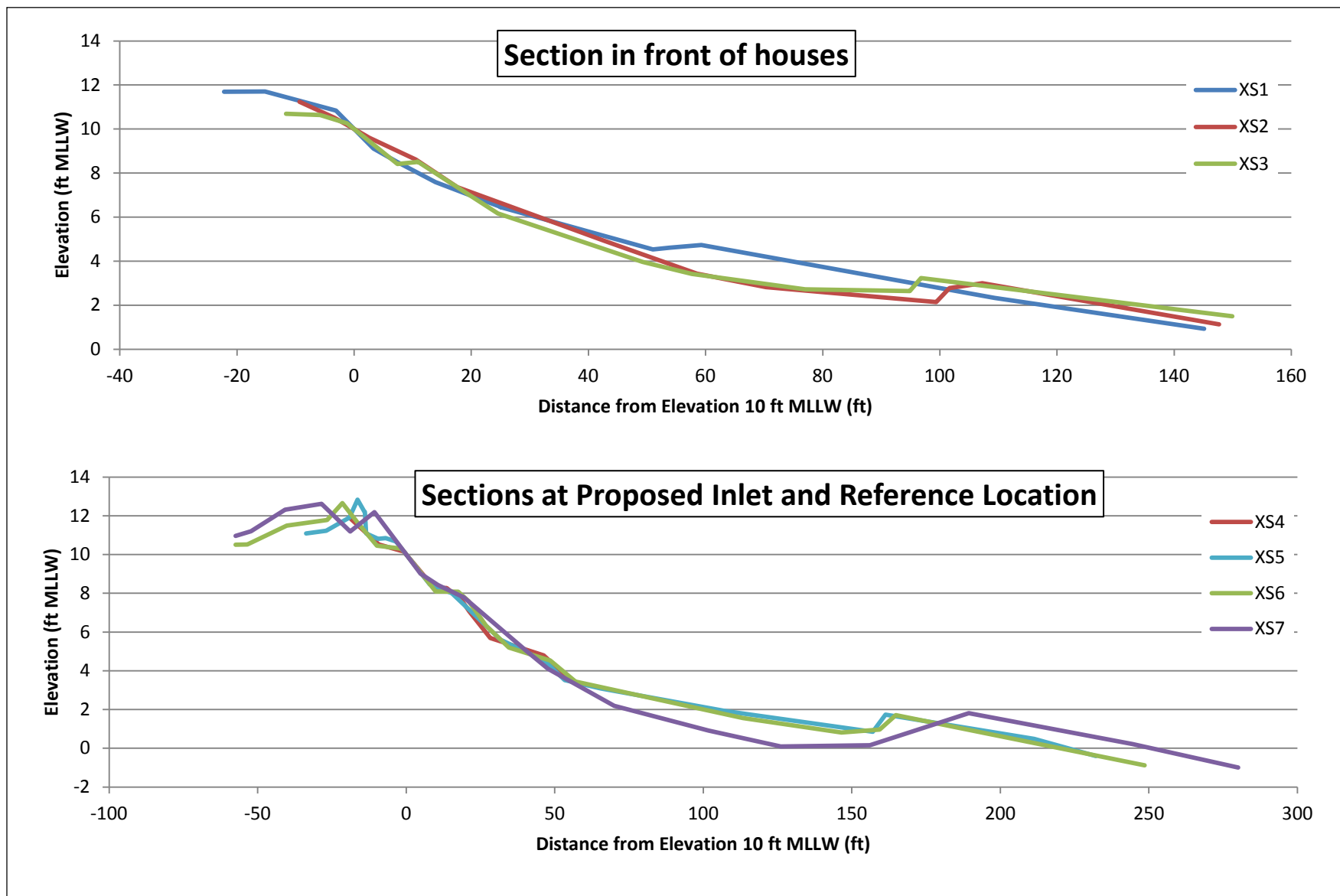


SOURCE: Puget Sound (CGS, PWA, 2010), Chesapeake Bay (Byrne et al., 1980) and New Zealand (Hume & Herdendorf, 1992)

Swan Lake Engineering Feasibility . 120062.00

Figure 13

Inlet cross-sectional area vs. inlet width and depth for all sites



SOURCE: CGS Survey Data, 2012

Swan Lake Engineering Feasibility . D120062.00

Figure 14

Surveyed beach profiles - top panel shows southern sections, bottom panel shows northern sections



Notes: Photo taken on May 14, 2012

Swan Lake Engineering Feasibility . 120062.00

Figure 15

Photograph of Swan Lake shore looking north – note the sand shoal separated from the predominantly cobble beach